

Different diagnostic values of imaging parameters to predict pseudoprogression in glioblastoma subgroups stratified by MGMT promoter methylation

Ra Gyoung Yoon¹ · Ho Sung Kim² · Wooyul Paik³ · Woo Hyun Shim² · Sang Joon Kim² · Jeong Hoon Kim⁴

Received: 9 December 2015 / Revised: 1 March 2016 / Accepted: 21 March 2016 / Published online: 5 April 2016
© European Society of Radiology 2016

Abstract

Objectives The aim of this study was to determine whether diffusion and perfusion imaging parameters demonstrate different diagnostic values for predicting pseudoprogression between glioblastoma subgroups stratified by O⁶-methylguanine-DNA methyltransferase (MGMT) promoter methylation status.

Methods We enrolled seventy-five glioblastoma patients that had presented with enlarged contrast-enhanced lesions on magnetic resonance imaging (MRI) one month after completing concurrent chemoradiotherapy and undergoing MGMT promoter methylation testing. The imaging parameters included 10 or 90 % histogram cutoffs of apparent diffusion coefficient

(ADC10), normalized cerebral blood volume (nCBV90), and initial area under the time signal-intensity curve (IAUC90). The results of the areas under the receiver operating characteristic curve (AUCs) with cross-validation were compared between MGMT methylation and unmethylation groups.

Results MR imaging parameters demonstrated a trend toward higher accuracy in the MGMT promoter methylation group than in the unmethylation group (cross-validated AUCs = 0.70–0.95 and 0.56–0.87, respectively). The combination of MGMT methylation status with imaging parameters improved the AUCs from 0.70 to 0.75–0.90 for both readers in comparison with MGMT methylation status alone. The probability of pseudoprogression was highest (95.7 %) when nCBV90 was below 4.02 in the MGMT promoter methylation group.

Conclusions MR imaging parameters could be stronger predictors of pseudoprogression in glioblastoma patients with the methylated MGMT promoter than in patients with the unmethylated MGMT promoter.

Key Points

- The glioblastoma subgroup was stratified according to MGMT promoter methylation status.
- Diagnostic values of diffusion and perfusion parameters for predicting pseudoprogression were compared.
- Imaging parameters showed higher diagnostic accuracy in the MGMT promoter methylation group.
- Imaging parameters were independent to MGMT promoter methylation status for predicting pseudoprogression.
- Imaging biomarkers might demonstrate different diagnostic values according to MGMT promoter methylation.

Ra Gyoung Yoon and Wooyul Paik contributed equally to this work.

✉ Ho Sung Kim
radhskim@gmail.com

Ra Gyoung Yoon
yoonrg@hanmail.net

¹ Department of Radiology, Catholic Kwandong University College of Medicine, Catholic Kwandong University International St. Mary's Hospital, 25, Simgok-ro 100beon-gil, Seo-gu, Incheon 22711, Republic of Korea

² Department of Radiology and Research Institute of Radiology, University of Ulsan College of Medicine, Asan Medical Center, 88, Olympic-ro 43-gil, Songpa-Gu, Seoul 05505, Republic of Korea

³ Department of Radiology, Dankook University Hospital, San 16-5, Anseo-dong, Dongnam-gu, Cheonan-si, Chungcheongnam-do 31116, Republic of Korea

⁴ Department of Neurosurgery, University of Ulsan College of Medicine, Asan Medical Center, 88, Olympic-ro 43-gil, Songpa-Gu, Seoul 05505, Republic of Korea

Keywords Glioblastoma · Pseudoprogression · MGMT promoter methylation · Diffusion-weighted imaging · Perfusion MR

Abbreviations

CCRT	Concurrent chemoradiotherapy
MR	Magnetic resonance
CBV	Cerebral blood volume
ADC	Apparent diffusion coefficient
MGMT	O ⁶ -methylguanine-DNA methyltransferase
DWI	Diffusion-weighted imaging
DSC	Dynamic susceptibility contrast-enhanced
DCE	Dynamic contrast-enhanced
IAUC	Initial area under the time–signal intensity curve
ROC	Receiver operating characteristic

Introduction

The evaluation of treatment response after concurrent chemoradiotherapy (CCRT) in glioblastoma has been advanced by the development of new standardized criteria regarding changes in tumour volume after therapy by the Response Assessment in Neuro-Oncology Working Group (RANO [1]). However, radiologic images obtained in the short time interval after CCRT still contain biases for treatment response evaluation due to increasing capillary permeability or tumour cell damage by therapy [2]. Several studies using perfusion magnetic resonance imaging (MRI) showed that changes in cerebral blood volume (CBV) within tumours that occur during the early radiotherapy course can predict pseudoprogression [3] and survival [4]. Others reported that the apparent diffusion coefficient (ADC) values are useful for distinguishing between high-grade glioma and normal tissue [5] and predicting treatment responses [6, 7]. However, the exact clinical impact of advanced MR imaging techniques including diffusion-weighted imaging (DWI), dynamic susceptibility contrast-enhanced (DSC) perfusion imaging, and dynamic contrast-enhanced (DCE) perfusion imaging has not been validated by large-series prospective studies conducted exclusively for post-treatment glioblastoma.

O⁶-methylguanine-DNA methyltransferase (MGMT) promoter methylation status was reported as a strong predictor of pseudoprogression and prognosis [8–10]. According to several reports about the correlation between MGMT promoter methylation status and imaging parameters, both of them should be considered when interpreting enlarged contrast-enhancing lesions on MR [3, 11]. Furthermore, the potential association between MGMT promoter methylation status and various imaging parameters may lead to the use of different diagnostic values in assessing treatment response in glioblastoma.

Our hypothesis is that diffusion and perfusion imaging parameters may demonstrate different diagnostic values for predicting pseudoprogression in glioblastoma patients according to MGMT promoter methylation status. The purpose of this study was to determine whether diffusion and perfusion

imaging parameters demonstrate different diagnostic values for predicting pseudoprogression between glioblastoma subgroups stratified by MGMT promoter methylation status.

Methods

Study population

Our institutional review board approved this retrospective study, and the requirement for informed consent from the study participants was waived. A retrospective review of our database identified 211 consecutive patients with pathologically proven glioblastoma between December 2010 and December 2014. Patients were included in our study if they met all of the following criteria: (a) underwent methylation-specific polymerase chain reaction (MS-PCR) of the tumour specimens to determine MGMT promoter methylation status; (b) underwent CCRT after surgery; (c) demonstrated new or progressively enlarged contrast-enhancing lesions on the follow-up MR at 4 weeks after CCRT, including DWI, DSC, and DCE perfusion MR; (d) underwent serial follow-up MR imaging with 2–3-month intervals; (e) not prescribed corticosteroid when MR imaging was performed; and (f) obtained adequate image acquisition and quality without susceptibility or motion artifacts.

We excluded 43 patients without MS-PCR results and six patients not treated with CCRT. Additionally, 16 patients were excluded due to the absence of DWI, DSC, or DCE images, corticosteroid treatment at the time of MR, or poor quality; another 71 patients with stable contrast-enhancing lesions after CCRT were also excluded. Finally, 75 patients were enrolled in this study. The 75 patients were dichotomized into MGMT promoter methylation and unmethylation groups. Fifteen of 75 patients were reported on previously, but this prior study evaluated the diagnostic performance of multiparametric imaging for simply identifying pseudoprogression [12]. The process flowchart for this study population is shown in Fig. 1.

MGMT promoter methylation analysis

MGMT promoter methylation status was evaluated after obtaining a specimen from surgery or biopsy. Unstained tissue slides made from paraffin-embedded blocks of tumour tissues were used to extract genomic DNA. MS-PCR with modifications was used to determine the DNA methylation status of the CpG islands at the MGMT promoter [13, 14]. The annealing temperature was 59 °C. Results from unqualified DNA that yielded uncertain PCR results were abandoned. For negative and positive controls, bisulfite-treated unmethylated and methylated control DNAs were used (Qiagen, Hilden, Germany). On 8 % polyacrylamide gels, the PCR products

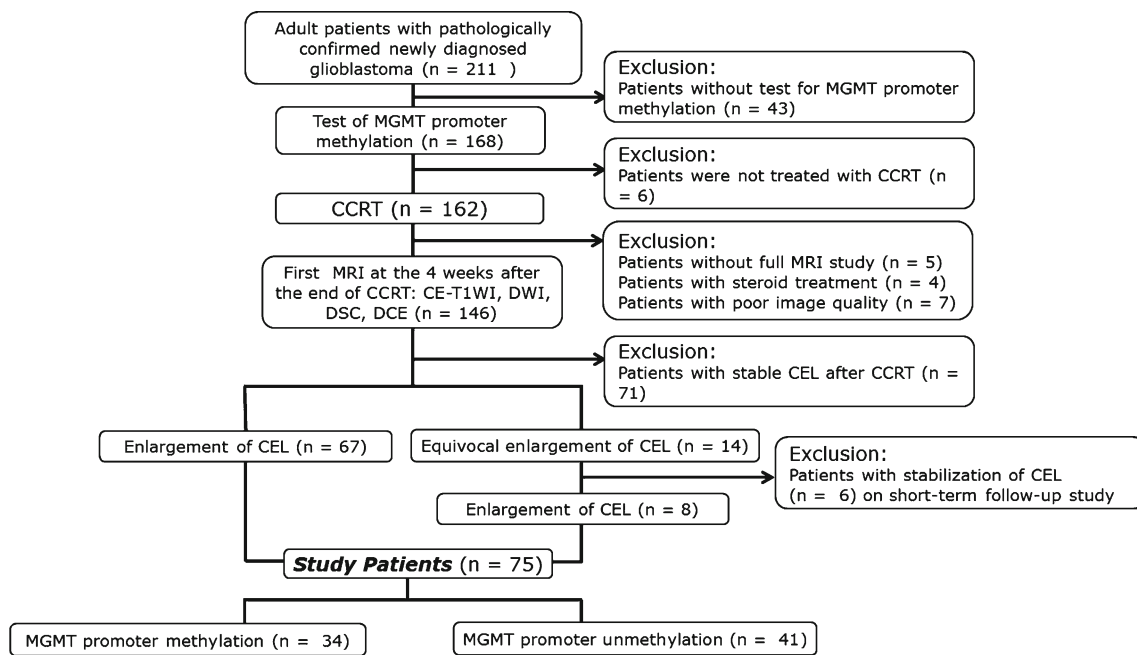


Fig. 1 Flowchart of the accrual process for the study population

were separated, stained with ethidium bromide, and inspected under ultraviolet illumination. For all steps, clinical information was processed in a blind manner using a computerized barcode.

Assessment

After the second-look surgery, nine cases were confirmed as true progression and three as pseudoprogression. If the second-look operation was unavailable, the progression was decided based on MR, clinical assessment, and steroid use. An experienced neuroradiologist (H.S.K.) blinded about clinical information independently reviewed all MR images. The clinico-radiological diagnoses of 27 cases of true progression and 36 cases of pseudoprogression were established by consensus between a neuro-oncologist (J.H.K., 20 years of clinical experience in neuro-oncology) and a neuroradiologist (H.S.K.) after completely reviewing images and medical charts. Clinical and radiologic assessments were carried out at pre-CCRT; 4 weeks after completion of the CCRT; during cycles 2, 4, and 6 of the adjuvant temozolomide therapy; and every 2 or 3 months thereafter. Pseudoprogression was defined using prespecified criteria [1], and confirmatory imaging was performed after two cycles of maintenance temozolomide therapy. The diagnosis of pseudoprogression was made when there was a decrease or stabilization of the contrast-enhancing lesions on subsequent serial follow-up MR images, and combined with no required change in treatment. This diagnosis allows a slight increase in contrast-enhancing lesions as long as no change in treatment occurs during this time period. A final diagnosis of true progression was made if the enhancing

lesions gradually increased on more than two serial follow-up MR images at 2-month intervals and were combined with clear neurologic deterioration attributable to enlarging contrast-enhancing lesions, causing a prompt change of treatment.

MR imaging protocol and image processing

The MR imaging studies were performed using a 3T system (Achieva; Philips Healthcare, Best, The Netherlands) with an 8-channel sensitivity-encoded head coil. The order of our brain tumour imaging protocol was as follows: T2-weighted imaging, fluid-attenuated inversion recovery imaging, DWI, non-enhanced T1-weighted imaging, DCE perfusion MR imaging, contrast-enhanced T1-weighted imaging, and DSC perfusion MR imaging. The rationale for the application of DCE imaging prior to DSC imaging is that preloading contrast agent injected during the DCE imaging can minimize T1 contrast agent leakage effects.

DWI was obtained in three orthogonal directions and combined into a trace image. Using these data, ADC maps were calculated using the b values of 0 and 1000 second/mm² on a voxel-by-voxel basis with the software incorporated into the MR imaging unit. Further information about the protocols of DWI, DSC, and DCE perfusion MR imaging are demonstrated in the supplementary material.

All MR imaging data were transferred from the MR imaging unit to an independent personal computer. A dedicated software package (Nordic ICE; Nordic Neuro Lab, Bergen, Norway) and in-house software (Matlab 2010b; Mathworks, Natick, MA) were used to obtain parametric perfusion maps.

The relative CBV (rCBV) was determined with the numeric integration of the time–signal intensity (SI) curve for DSC MR imaging after correcting contrast agent leakage. On a pixel-by-pixel basis, normalized CBV (nCBV) maps were computed by dividing the individual rCBV value by an unaffected white matter rCBV value. For DCE MR imaging, the SI was normalized to the percentage change in comparison with the baseline SI value. Then, we calculated the initial area under the time SI curves (IAUCs) at 30 seconds after contrast agent administration using the trapezoidal integration of the normalized SI with time over the first 30 seconds after contrast agent arrival in the enhancing voxels of interest. We chose this model-free parameter because of our intention to maximally decrease the dependence on complex modelling of the pharmacokinetics, which can be sensitive to noise [15].

Image analysis

Intermodality coregistration and enhancing lesion segmentation The ADC, nCBV, and IAUC maps were coregistered to each of the three-dimensional contrast-enhanced T1-weighted images. Intermodality coregistrations were performed using a non-linear transformation. For the quantitative analysis of data acquired from the DWI, DSC, and DCE MR imaging, a neuroradiology expert (H.S.K.; reader 1) and a neuroradiology fellow (J.E.P. with 5 years of experience in radiology; reader 2) segmented the entire volumes of the contrast-enhancing lesions on the coregistered contrast-enhanced T1 weighted images using a semi-automated adaptive threshold technique so that all pixels above a threshold value were taken.

DWI analysis For the quantitative DWI analyses, the 10th percentile of the histogram cutoff for the ADC value (ADC10) was calculated. This parameter was selected because the 10th percentile parameter is analogous to the minimum value, which is commonly used with the hot-spot method.

DSC and DCE MR imaging analyses For the cumulative nCBV and IAUC histogram parameters, the 90th percentile cutoffs were derived (nCBV90 and IAUC90, respectively). This kind of histogram parameter is more powerful than the mean and maximum values of the overall histogram for identifying areas where tumorous lesions are intermingled with treatment-associated changes and are less affected by random statistical fluctuations [16].

Statistical analyses

The imaging data were initially assessed for normality using the Kolmogorov-Smirnov test. To assess differences in demographic data between the MGMT promoter methylation and

unmethylation groups, the Student's *t* test for continuous variables and the chi-squared test for categorical variables were used.

In the subgroup analyses stratified by MGMT promoter methylation, differences in the mean values of the imaging parameters between the two groups were assessed using the Student's *t* test. Receiver operating characteristic (ROC) curve analysis was performed on each imaging parameter to determine the optimum cutoff for differentiating between the two groups and to compare the area under the ROC curve (AUC). Bonferroni correction was used to control for multiple comparisons. Using the same population to select classifiers and estimate error rates can overfit the diagnostic performances, so imaging parameters were further evaluated using leave-one-out cross-validation. Using this method, all study patients (except for one patient) were used as the training set, and the prediction error was assessed for the excluded test set. This procedure was repeated until every case was used once as the test set.

Multivariable logistic regression modelling was used to estimate the odds ratios for the association between the combination of MGMT promoter methylation and imaging parameters with the final diagnosis. Cross-validation was also used to determine the association between the imaging parameters and final diagnosis. The ROC-based optimum cutoff values, which were calculated based on the highest Youden index [17], were used as exploratory analyses to dichotomize subgroups of each imaging parameter. The results are considered significant at $P < 0.05$ and corrected for the number of comparisons.

Inter-reader agreement was assessed using the intraclass correlation coefficient (ICC) with 95 % confidence intervals and by applying a two-way ICC with a random rater's assumption. Instances of $P < 0.05$ were considered to indicate significant statistical differences. Statistical analyses were performed using SPSS (version 21.0; SPSS, Chicago, IL) and R version 2.15.3 (R Project for Statistical Computing; <http://www.r-project.org>).

Results

Clinical parameters of subgroups

Among 75 patients, 34 (45.3 %) were classified to the MGMT promoter methylation group and 41 (54.7 %) to the MGMT promoter unmethylation group. No clinical parameters were significantly different between the two groups (Table 1). Contrast-enhancing lesion-related clinical symptoms were presented in 17 (50.0 %) of 34 MGMT promoter methylation patients and 28 (68.3 %) of 41 MGMT promoter methylation patients ($P = 0.170$). In total, 25 cases (73.5 %) of

Table 1 Demographic data for both the MGMT promoter methylated and unmethylated glioblastoma subgroups

Variables	MGMT methylation group (n = 34)	MGMT unmethylation group (n = 41)	p value
Sex			0.967
No. of male patients	16 (47.1 %)	18 (43.9 %)	
No. of female patients	18 (52.9 %)	23 (56.1 %)	
Age (y)*	53.2 ± 12.3	53.9 ± 12.9	0.851
KPS*	94.7 ± 7.5	92.9 ± 6.5	0.605
CEL-related clinical symptom	17 (50.0 %)	28 (68.3 %)	0.170
Surgical extent before CCRT			0.962
Biopsy or partial resection	14 (41.2 %)	16 (39.0 %)	
Gross total resection	20 (58.8 %)	25 (61.0 %)	
Mean radiation dose at CCRT (Gy)	59.4 ± 2.1	59.7 ± 1.9	0.430
Mean interval between CCRT and enlarged CEL (wks)	11.2 ± 3.6	10.3 ± 3.5	0.279

KPS = Karnofsky performance status; CEL = contrast-enhancing lesion; CCRT = concurrent chemoradiotherapy; Gy = gray

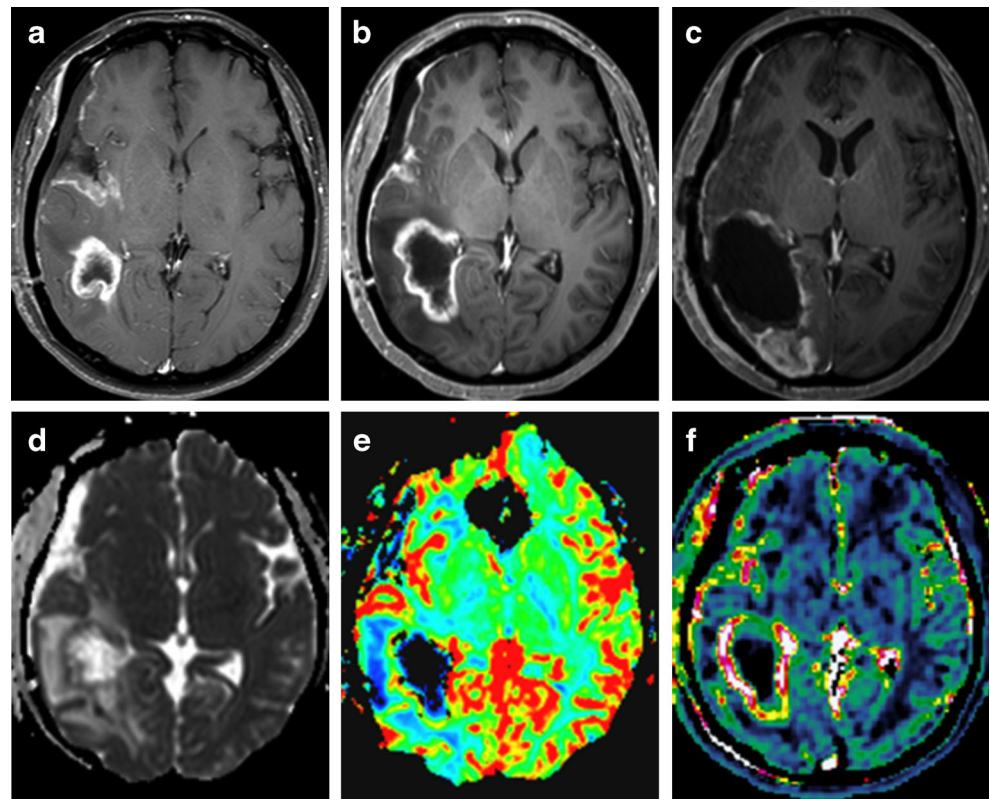
*Data are expressed as the mean ± standard deviation

pseudoprogression and nine cases (26.5 %) of true progression were in the MGMT promoter methylation group, while the MGMT promoter unmethylation group included 14 cases (34.1 %) of pseudoprogression and 27 cases (65.9 %) of true progression. This difference was statistically significant ($P=0.002$) according to the chi-squared test. Representative cases are shown in Figs. 2 and 3.

Diagnostic accuracy of the imaging parameters in the subgroups

In the MGMT promoter methylation group, the mean values of the DWI, DSC, and DCE MR imaging parameters were significantly different between the true progression and pseudoprogression groups for both readers (corrected

Fig. 2 Images obtained from a 38-year-old female glioblastoma patient with MGMT promoter methylation and true tumour progression. **a** Contrast-enhanced T1-weighted image obtained 7 weeks after CCRT. A necrotic contrast-enhancing lesion can be observed in the right temporal lobe. **b, c** Contrast-enhanced T1-weighted image obtained 15 weeks after CCRT and 2 days after surgery for a recurrent tumour; **b** in this panel, the contrast-enhancing lesion is enlarged. The ADC map (**d**) shows restricted diffusion in the corresponding contrast-enhancing lesion shown in (**b**). Both the nCBV (**e**) and IAUC (**f**) maps show increased perfusion pixel values in the corresponding contrast-enhancing lesion shown in (**b**), suggesting true tumour progression (i.e., true positive)



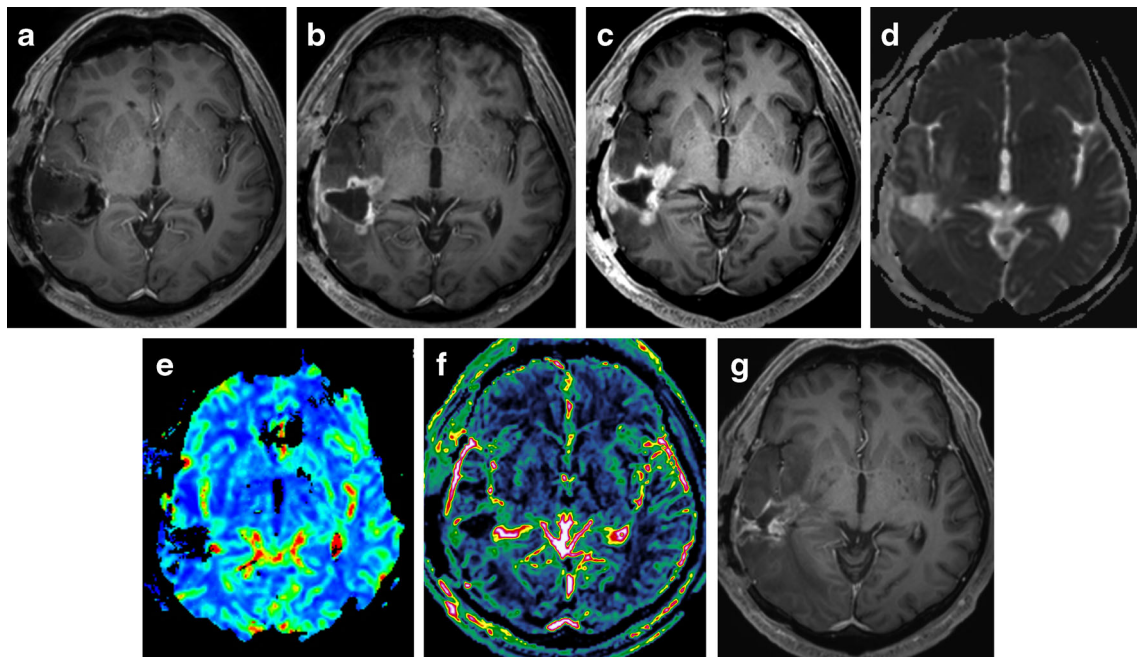


Fig. 3 Images obtained from a 59-year-old male glioblastoma patient with MGMT promoter unmethylation and pseudoprogression. **a, b** Contrast-enhanced T1-weighted images obtained before and 5 weeks after CCRT. A newly developed contrast-enhancing lesion is seen around the surgical cavity. **c** Contrast-enhanced T1-weighted images obtained 10 weeks after CCRT. The size of the contrast-enhancing lesion increased. The ADC map (**d**) shows equivocal finding of

restricted diffusion in the corresponding contrast-enhancing lesion shown in (**c**). Both the nCBV (**e**) and IAUC (**f**) maps show no increase of perfusion pixel values in the corresponding contrast-enhancing lesion shown in (**c**), suggesting pseudoprogression. **g** Contrast-enhanced T1-weighted images obtained 20 weeks after CCRT. The contrast-enhancing lesion is stabilized, confirming pseudoprogression

$P = .001-.006$ for reader 1; corrected $P = .001-.039$ for reader 2). In the MGMT promoter unmethylated group, the mean values of the nCBV90 and IAUC90 values were significantly different between the two groups for both readers (corrected $P = .001-.003$ for both readers). However, the mean ADC10

values were not significantly different between groups for both readers (Table 2 and Fig. 4).

On the ROC curve analysis, the AUCs were highest for nCBV90 derived from DSC MR imaging and lowest for the ADC10 derived from DWI in both groups for both readers

Table 2 Comparison of imaging parameters between cases of true tumour progression and pseudoprogression in the subgroups stratified by MGMT promoter methylation

Reader and Parameter	MGMT methylation group (n = 34)			MGMT unmethylation group (n = 41)		
	True progression (n = 9)	Pseudoprogression (n = 25)	Corrected <i>p</i> value	True progression (n = 27)	Pseudoprogression (n = 14)	Corrected <i>p</i> value
Reader 1						
ADC10 ($10^{-3} \text{ mm}^2 \text{ sec}^{-1}$)	0.92 ± 0.09	1.04 ± 0.08	0.006	0.93 ± 0.05	0.96 ± 0.08	0.276
nCBV90	5.34 ± 1.26	2.69 ± 0.95	<0.001	4.48 ± 1.47	2.68 ± 0.78	0.001
IAUC90	23.58 ± 1.62	19.83 ± 3.23	0.006	22.88 ± 2.73	19.65 ± 3.00	0.003
Reader 2						
ADC10 ($10^{-3} \text{ mm}^2 \text{ sec}^{-1}$)	0.92 ± 0.09	1.01 ± 0.09	0.039	0.94 ± 0.07	0.96 ± 0.07	0.862
nCBV90	5.50 ± 1.14	2.80 ± 0.93	<0.001	4.37 ± 1.32	2.55 ± 0.90	0.001
IAUC90	23.81 ± 2.05	19.57 ± 2.93	0.003	22.64 ± 2.32	19.56 ± 3.20	0.003

ADC10 = 10th percentile cutoff value of ADC; nCBV90 = 90th percentile cutoff value of nCBV; IAUC90 = 90th percentile cutoff value of IAUC

*Data are expressed as the median with maximum and minimum in the parentheses

For comparison of tumour progression vs. pseudoprogression, the *P* values were corrected for multiple comparisons using Bonferroni correction

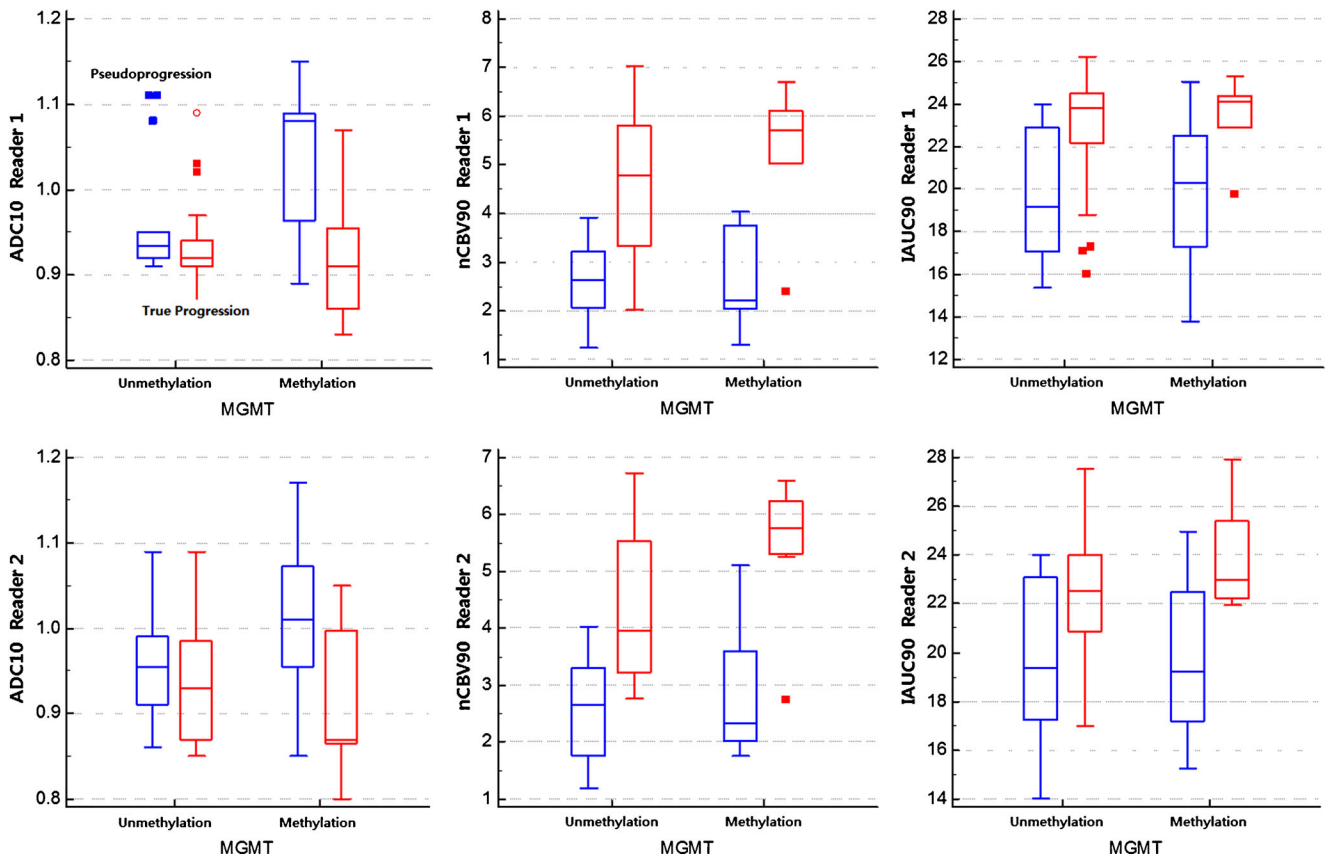


Fig. 4 Box-and-Whisker plots for comparison of the values of the imaging parameters between true progression and pseudoprogession in subgroups stratified by MGMT promoter methylation for both readers

(Table 3). For comparing two perfusion parameters in terms of differentiating true progression from pseudoprogession, the nCBV90 derived from DSC MR imaging showed a higher AUC than the IAUC90 derived from DCE perfusion MR imaging in both MGMT methylation and unmethylation groups

for both readers. However, these results were not statistically significant (Table 3). All of the three imaging parameters demonstrated a trend towards higher AUCs in the MGMT promoter methylation group than in the MGMT promoter unmethylation group for differentiating true progression from

Table 3 Diagnostic performances of the imaging parameters for predicting pseudoprogession in the subgroups stratified by MGMT promoter methylation

Reader and Parameter	MGMT methylation group (n = 34)			MGMT unmethylation group (n = 41)		
	AUC	SE of AUC	95 % CI of AUC	AUC	SE of AUC	95 % CI of AUC
Reader 1						
ADC10 ($10^{-3} \text{ mm}^2 \text{ sec}^{-1}$)	0.85	0.07	0.69, 0.95	0.65	0.09	0.49, 0.79
nCBV90	0.95	0.05	0.81, 0.99	0.85	0.06	0.71, 0.95
IAUC90	0.86	0.07	0.70, 0.96	0.81	0.07	0.66, 0.92
Reader 2						
ADC10 ($10^{-3} \text{ mm}^2 \text{ sec}^{-1}$)	0.76	0.10	0.59, 0.89	0.60	0.09	0.43, 0.75
nCBV90	0.95	0.05	0.82, 0.99	0.87	0.06	0.73, 0.96
IAUC90	0.86	0.06	0.70, 0.96	0.77	0.09	0.61, 0.88

AUC = area under the ROC curve; SE = standard error; CI = confidence interval; ADC10 = 10th percentile cutoff value of ADC; nCBV90 = 90th percentile cutoff value of nCBV; IAUC90 = 90th percentile cutoff value of IAUC. Parentheses indicate the 95 % confidence interval

pseudoprogression. On the leave-one-out cross-validation, the cross-validated AUCs and the accuracies of the imaging parameters demonstrated similar trends, as did the ROC curve analyses using the same training and validation sets (Table 4 and Fig. 5).

Independence and added value of the imaging parameters to MGMT promoter methylation status

Exploratory analyses using the optimum cutoff values based on the highest Youden index were performed to test the independence and added value of the imaging parameters to the MGMT promoter methylation status for predicting pseudoprogression. On multivariate logistic regression analyses using MGMT promoter methylation status, all of the three imaging parameters independently influenced the incidence of pseudoprogression ($P = .004$ – $.001$ for reader 1; $P = .041$ – $.001$ for reader 2, respectively). The combination of MGMT promoter methylation status with each imaging parameters improved the AUCs from 0.70 to 0.75–0.90 for both readers in comparison with MGMT promoter methylation status alone (Table 5). The cross-validated AUCs and accuracies of the imaging parameters demonstrated similar trends, as did the ROC curve analyses using the same training and validation sets (Table 6).

Probability of pseudoprogression using the decision tree

A diagnostic decision tree was constructed based on the exploratory analyses using our own optimum cutoff values (Fig. 6). The probability of pseudoprogression was highest (95.7 %) when nCBV90 was below 4.02 in the MGMT promoter methylation group and lowest (0 %) when nCBV90 was above 4.02 in the MGMT promoter unmethylation group. The probability of pseudoprogression was 90.0 % when the

Fig. 5 Leave-one-out cross-validation used to determine the diagnostic accuracy of DWI, DSC, and DCE MR imaging for differentiating true tumour progression from pseudoprogression in subgroups stratified by MGMT promoter methylation for both readers **a** MGMT promoter methylated group; **b** MGMT promoter unmethylated group

ADC10 was above 0.94 in the MGMT promoter methylation group.

Inter-reader agreement for measuring imaging parameters

The ICCs were 0.71, 0.86, and 0.74 for the calculations of ADC10, nCBV90, and IAUC90, respectively.

Discussion

In our study, we found that the DSC and DCE perfusion parameters demonstrated significant differences between true progression and pseudoprogression in glioblastoma demonstrating either MGMT promoter methylation or unmethylation, although the ADC value demonstrated a significant difference between these two entities in the MGMT promoter methylation group only. Moreover, diffusion and perfusion MR imaging parameters demonstrated better diagnostic performance to predict pseudoprogression in the MGMT promoter methylation group compared to the unmethylation group. When comparing perfusion parameters obtained with both DCE and DSC techniques, we found that the best overall diagnostic accuracy to predict pseudoprogression was achieved with the combination of DSC perfusion MR imaging and MGMT promoter methylation. These results suggest that the MR imaging protocol that includes DSC perfusion MR imaging is most efficient in the prediction of pseudoprogression in the MGMT promoter methylation

Table 4 Leave-one-out cross-validation of the imaging parameters in the subgroups stratified by MGMT promoter methylation

	MGMT methylation group (n = 34)		MGMT unmethylation group (n = 41)	
	Cross-validated AUC	Cross-validated accuracy	Cross-validated AUC	Cross-validated accuracy
Reader 1				
ADC10	0.80	80.8 %	0.61	67.5 %
nCBV90	0.95	97.6 %	0.83	69.0 %
IAUC90	0.88	87.4 %	0.79	76.7 %
Reader 2				
ADC10	0.70	75.1 %	0.56	32.5 %
nCBV90	0.94	93.8 %	0.86	84.1 %
IAUC90	0.87	74.9 %	0.71	74.5 %

AUC = area under the ROC curve; ADC10 = 10th percentile cutoff value of ADC; nCBV90 = 90th percentile cutoff value of nCBV; and IAUC90 = 90th percentile cutoff value of IAUC

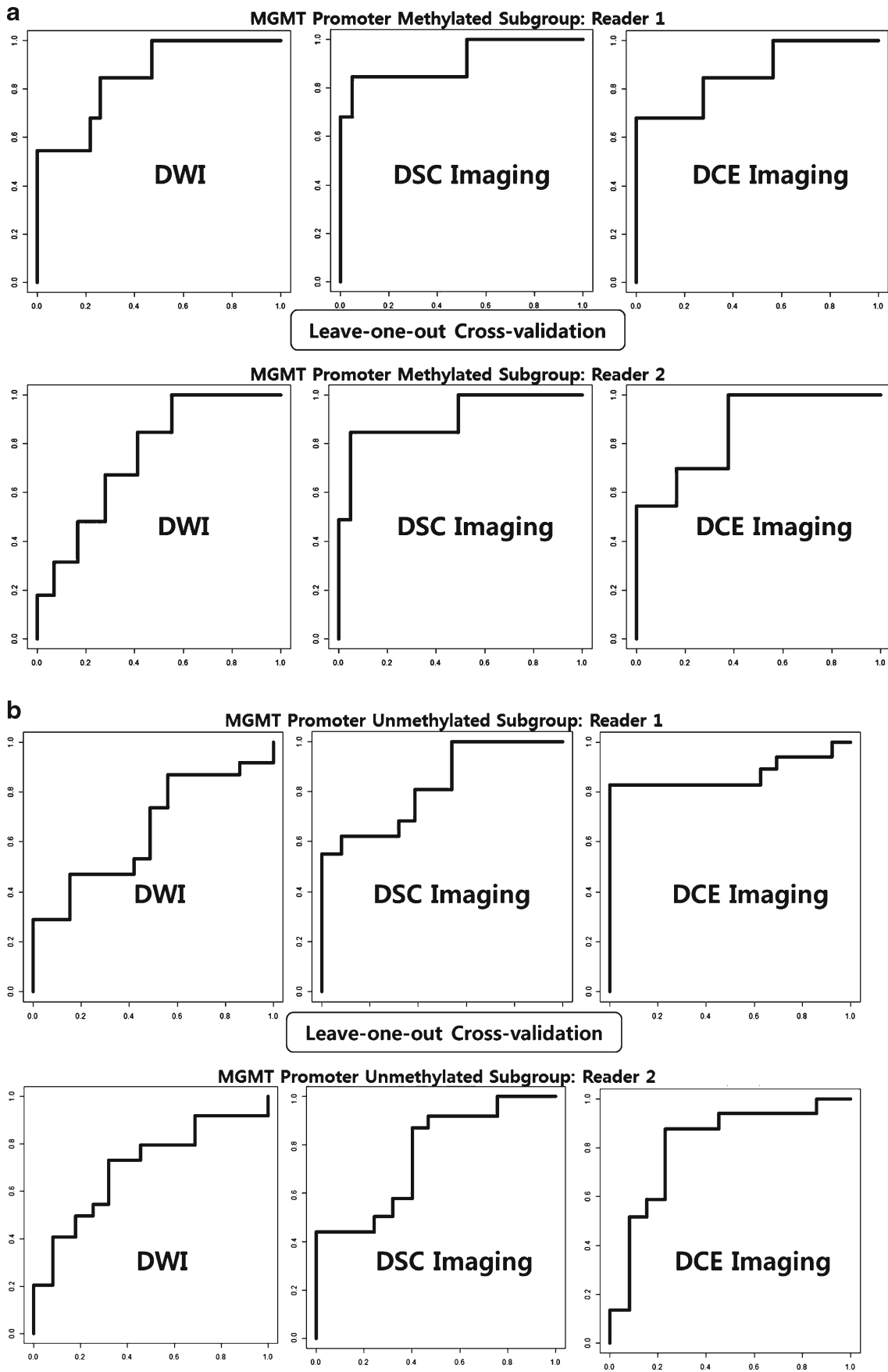


Table 5 Multivariate logistic regression analysis for predicting pseudoprogression using MGMT promoter methylation alone and in combination with the indicated imaging parameters for both readers

	Odds ratio of MGMT methylation	Odds ratio of imaging parameter	P value of imaging parameter	AUC
MGMT promoter methylation	5.36 (1.97–14.54)			0.70
Reader 1				
MGMT promoter methylation + $ADC_{10} \geq 0.94 \times 10^{-3} \text{ mm}^2 \text{ sec}^{-1}$	4.22 (1.46–12.24)	4.70 (1.64–13.45)	0.004	0.78
MGMT promoter methylation + $nCBV_{90} < 4.02$	22.17 (2.70–182.21)	89.27 (9.62–828.74)	<0.001	0.90
MGMT promoter methylation + $IAUC_{90} < 23.39$	6.64 (1.91–23.13)	16.37 (4.09–65.47)	0.001	0.84
Reader 2				
MGMT promoter methylation + $ADC_{10} \geq 0.96 \times 10^{-3} \text{ mm}^2 \text{ sec}^{-1}$	4.62 (1.65–12.94)	2.88 (1.04–7.96)	0.041	0.75
MGMT promoter methylation + $nCBV_{90} < 2.76$	4.13 (1.29–13.22)	34.15 (4.11–283.97)	0.001	0.84
MGMT promoter methylation + $IAUC_{90} < 20.02$	5.22 (1.55–17.57)	26.72 (5.21–137.06)	0.001	0.85

AUC = area under the ROC curve; ADC_{10} = 10th percentile cutoff value of ADC; $nCBV_{90}$ = 90th percentile cutoff value of nCBV; and $IAUC_{90}$ = 90th percentile cutoff value of IAUC.

Parentheses indicate the 95 % confidence interval

patient, as compared with that which includes DCE perfusion MR imaging. On the multivariate analysis, diffusion and perfusion MR imaging parameters were independent to MGMT promoter methylation status for predicting pseudoprogression, and provided added value in terms of diagnostic accuracy. Among the three imaging parameters, nCBV90 showed the highest diagnostic accuracy for predicting pseudoprogression in both MGMT promoter methylation and unmethylation groups. Lastly, the probability of pseudoprogression was highest (22 of 23 patients; 95.7 %) when the nCBV90 was below 4.02 in the MGMT promoter methylation group on our exploratory analyses. These results imply that the role of the imaging parameters for assessing treatment response could be limited by MGMT promoter unmethylation, which leads to predetermined chemoresistance of the tumour, regardless of other tumour microenvironments estimated using various imaging parameters. However, imaging parameters (especially

perfusion parameters) could provide added value to MGMT promoter methylation status for predicting pseudoprogression in the MGMT promoter methylation group, which reflects the early treatment response to CCRT. This suggests that tumour vascularity and permeability might also be important for the treatment response in glioblastoma demonstrating MGMT promoter methylation.

In contrast to our results, a previous study reported that the rCBV demonstrates more predictability in the MGMT promoter unmethylation group than in the methylation group [3]. However, this previous study demonstrated a remarkable incidence of true progression in their MGMT promoter unmethylation group, whereas we observed a remarkable incidence of pseudoprogression in our MGMT promoter methylation group. Besides, we used the histogram parameters of nCBV from the entire corresponding contrast-enhancing lesion instead of the “hot-spot” method. Regarding the DCE

Table 6 Cross-validation of MGMT promoter methylation alone in combination with the indicated imaging parameters for both readers

	Cross-validated AUC	Cross-validated accuracy
MGMT promoter methylation	0.69	68.9 %
Reader 1		
MGMT promoter methylation + $ADC_{10} \geq 0.94 \times 10^{-3} \text{ mm}^2 \text{ sec}^{-1}$	0.79	73.3 %
MGMT promoter methylation + $nCBV_{90} < 4.02$	0.90	81.5 %
MGMT promoter methylation + $IAUC_{90} < 23.39$	0.85	77.1 %
Reader 2		
MGMT promoter methylation + $ADC_{10} \geq 0.96 \times 10^{-3} \text{ mm}^2 \text{ sec}^{-1}$	0.74	66.9 %
MGMT promoter methylation + $nCBV_{90} < 2.76$	0.84	77.5 %
MGMT promoter methylation + $IAUC_{90} < 20.02$	0.86	77.1 %

AUC = area under the ROC curve; ADC_{10} = 10th percentile cutoff value of ADC; $nCBV_{90}$ = 90th percentile cutoff value of nCBV; and $IAUC_{90}$ = 90th percentile cutoff value of IAUC.

Parentheses indicate 95 % confidence interval

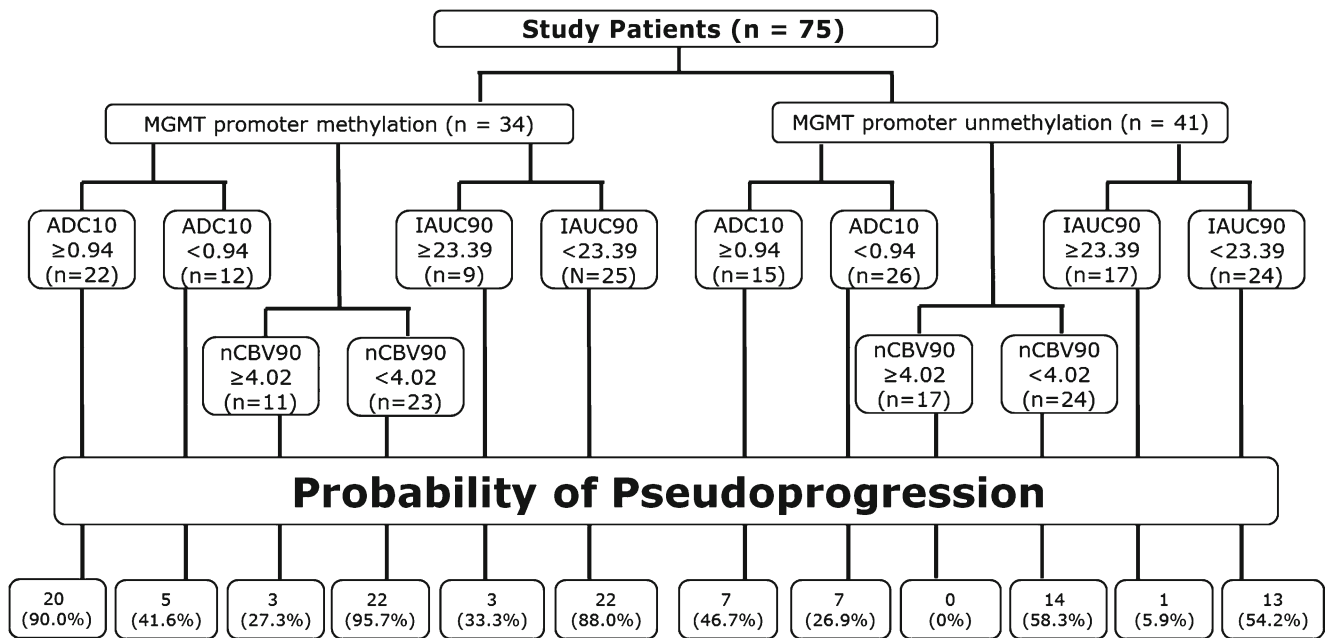


Fig. 6 Diagnostic decision tree constructed based on exploratory analyses that used the combination of MGMT promoter methylation status with our own optimum cutoff values of the imaging parameters to determine the probability of pseudoprogession

MR, to the best of our knowledge, no previous studies reported the diagnostic performance of DCE MR imaging parameters for predicting pseudoprogession in glioblastoma stratified by MGMT promoter methylation. We found a similar trend with the results of DSC MR imaging, which demonstrated a higher diagnostic performance for IAUC90 in the MGMT methylation group. Therefore, we suggest that perfusion imaging parameters could provide added diagnostic value for predicting pseudoprogession in the MGMT promoter methylation group.

Although it remains unclear as to why different diagnostic values of the imaging parameters were observed between MGMT promoter methylation and unmethylation groups, one possible explanation is that the higher diagnostic performance of the imaging parameters in the MGMT promoter methylation group might be associated with a higher proportion of pseudoprogession in the MGMT methylation group, whereas a relatively even distribution of true progession and pseudoprogession is seen in the unmethylation group. However, even if the correlation between the MGMT promoter methylation status and incidence of pseudoprogession may lead to a decrease in the power of the relationship between imaging parameters and pseudoprogession, there was a significant relationship between the three imaging parameters and the incidence of pseudoprogession in the MGMT promoter methylation group.

Interestingly, the combination of MGMT methylation and perfusion parameters provided additional diagnostic value for predicting pseudoprogession compared to the combination of MGMT promoter methylation and diffusion parameter. A previous study proposed that tumours with low ADC values can

be enriched in MGMT promoter-methylated tumour cells [18], in which elevated minimum ADC values and/or lower mean ADC values were associated with MGMT promoter methylation status. Therefore, the lowest diagnostic accuracy of ADC for predicting pseudoprogession in subgroups might be attributed to the stronger association between MGMT promoter methylation status and ADC values than those of perfusion parameters. Regarding the perfusion MR, one previous study reported that the MGMT promoter methylation status in glioblastoma is not associated with the rCBV ratio [19]. In contrast, a recent study suggested that the MGMT protein modulates angiogenesis of glioblastoma by changing the levels of vascular endothelial growth factor receptors [20], and accordingly, different rCBV ratios could be expected with respect to the MGMT methylation status of the tumour. Thereby, it may explain why the diagnostic values of the perfusion parameters differed between the MGMT promoter methylation and unmethylation groups in our study.

On our exploratory analyses, we found that the combination of MGMT promoter methylation and nCBV90 below 4.02 can predict pseudoprogession with a probability of 95.7 %. A previous study also reported that there is a 91.3 % probability of pseudoprogession in patients with the methylated MGMT promoter if the first MR image after CCRT shows enlargement of the enhancing lesion [8]. Therefore, these results also imply that the setting of the molecular profile and imaging parameters may reflect treatment-induced blood–brain barrier disruption, which is related to the efficacy of CCRT.

Our study has several limitations. First, it was a retrospective study with relatively small number of populations which

causes uneven categorization of patient groups. Therefore, a further prospective study is needed to validate our results. Second, the pathophysiological mechanisms that underlie the different diagnostic values of the imaging parameters between the two subgroups remain unclear, and future investigation with an experimental approach for tumorigenesis and genomics is warranted.

In conclusion, diffusion and perfusion imaging parameters may demonstrate different diagnostic values for predicting pseudoprogression in glioblastoma subgroups stratified by MGMT promoter methylation status. Our results suggest that MR imaging parameters could be stronger predictors of pseudoprogression in glioblastoma patients with the methylated MGMT promoter than in patients with the unmethylated MGMT promoter. Among the three imaging parameters, DSC perfusion MR imaging shows the highest diagnostic accuracy for predicting pseudoprogression in both MGMT promoter methylation and unmethylation groups. Therefore, the addition of DSC perfusion MR imaging may provide increased accuracy in glioblastoma demonstrating MGMT promoter methylation for predicting pseudoprogression.

Acknowledgments The scientific guarantor of this publication is Prof. Sang Joon Kim. This research was supported by Basic Science Research Program through the National Research Foundation of Korea (NRF) funded by the Ministry of Education, Science and Technology (grant number: NRF-2014R1A2A2A01004937). The Institutional Review Board approved our human study (The Institutional Review Board of Asan Medical Center [<http://eirb.amc.seoul.kr>]: S2014-2090-0001). Written informed consent was waived by the Institutional Review Board. Methodology: retrospective, diagnostic or prognostic study, performed at one institution. The authors thank the Biomedical Imaging Infrastructure, Department of Radiology, Asan Medical Center for the technical support of image processing. Some subjects or cohorts have been previously reported in Park JE, Kim HS, Goh MJ, Kim SJ, Kim JH. Pseudoprogression in patients with glioblastoma: assessment by using volume-weighted voxel-based multiparametric clustering of MR imaging data in an independent test set. *Radiology* 2015 Jun;275(3):792–802.

References

- Wen PY, Macdonald DR, Reardon DA et al (2010) Updated response assessment criteria for high-grade gliomas: response assessment in neuro-oncology working group. *J Clin Oncol* 28:1963–1972
- Brandes AA, Rigon A, Zampieri P et al (1998) Carboplatin and teniposide concurrent with radiotherapy in patients with glioblastoma multiforme: a phase II study. *Cancer* 82:355–361
- Kong DS, Kim ST, Kim EH et al (2011) Diagnostic dilemma of pseudoprogression in the treatment of newly diagnosed glioblastomas: the role of assessing relative cerebral blood flow volume and oxygen-6-methylguanine-DNA methyltransferase promoter methylation status. *AJNR Am J Neuroradiol* 32:382–387
- Catalaa I, Henry R, Dillon WP et al (2006) Perfusion, diffusion and spectroscopy values in newly diagnosed cerebral gliomas. *NMR Biomed* 19:463–475
- Castillo M, Smith JK, Kwoc L, Wilber K (2001) Apparent diffusion coefficients in the evaluation of high-grade cerebral gliomas. *AJNR Am J Neuroradiol* 22:60–64
- Pope WB, Kim HJ, Huo J et al (2009) Recurrent glioblastoma multiforme: ADC histogram analysis predicts response to bevacizumab treatment. *Radiology* 252:182–189
- Pope WB, Lai A, Mehta R et al (2011) Apparent diffusion coefficient histogram analysis stratifies progression-free survival in newly diagnosed bevacizumab-treated glioblastoma. *AJNR Am J Neuroradiol* 32:882–889
- Brandes AA, Franceschi E, Tosoni A et al (2008) MGMT promoter methylation status can predict the incidence and outcome of pseudoprogression after concomitant radiochemotherapy in newly diagnosed glioblastoma patients. *J Clin Oncol* 26:2192–2197
- Brandes AA, Tosoni A, Franceschi E et al (2009) Recurrence pattern after temozolomide concomitant with and adjuvant to radiotherapy in newly diagnosed patients with glioblastoma: correlation with MGMT promoter methylation status. *J Clin Oncol* 27:1275–1279
- Weller M, Tabatabai G, Kastner B et al (2015) MGMT promoter methylation is a strong prognostic biomarker for benefit from dose-intensified temozolomide rechallenge in progressive glioblastoma: the DIRECTOR trial. *Clin Cancer Res* 21:2057–2064
- Drabycz S, Roldan G, de Robles P et al (2010) An analysis of image texture, tumor location, and MGMT promoter methylation in glioblastoma using magnetic resonance imaging. *NeuroImage* 49:1398–1405
- Park JE, Kim HS, Goh MJ, Kim SJ, Kim JH (2015) Pseudoprogression in patients with glioblastoma: assessment by using volume-weighted voxel-based multiparametric clustering of MR imaging data in an independent test set. *Radiology* 275:792–802
- Esteller M, Garcia-Foncillas J, Andion E et al (2000) Inactivation of the DNA-repair gene MGMT and the clinical response of gliomas to alkylating agents. *N Engl J Med* 343:1350–1354
- Esteller M, Hamilton SR, Burger PC, Baylin SB, Herman JG (1999) Inactivation of the DNA repair gene O6-methylguanine-DNA methyltransferase by promoter hypermethylation is a common event in primary human neoplasia. *Cancer Res* 59:793–797
- Evelhoch JL, LoRusso PM, He Z et al (2004) Magnetic resonance imaging measurements of the response of murine and human tumors to the vascular-targeting agent ZD6126. *Clin Cancer Res* 10:3650–3657
- Kim HS, Goh MJ, Kim N, Choi CG, Kim SJ, Kim JH (2014) Which combination of MR imaging modalities is best for predicting recurrent glioblastoma? Study of diagnostic accuracy and reproducibility. *Radiology* 273:831–843
- Youden WJ (1950) Index for rating diagnostic tests. *Cancer* 3:32–35
- Wong AJ, Bigner SH, Bigner DD, Kinzler KW, Hamilton SR, Vogelstein B (1987) Increased expression of the epidermal growth factor receptor gene in malignant gliomas is invariably associated with gene amplification. *Proc Natl Acad Sci U S A* 84:6899–6903
- Moon WJ, Choi JW, Roh HG, Lim SD, Koh YC (2012) Imaging parameters of high grade gliomas in relation to the MGMT promoter methylation status: the CT, diffusion tensor imaging, and perfusion MR imaging. *Neuroradiology* 54:555–563
- Chahal M, Xu Y, Lesniak D et al (2010) MGMT modulates glioblastoma angiogenesis and response to the tyrosine kinase inhibitor sunitinib. *Neuro-Oncology* 12:822–833